

1 **Quantitative analysis of spore shapes improves identification of fungi**

2 Alexander Ordynets<sup>1\*</sup>, Sarah Keßler<sup>1</sup>, Ewald Langer<sup>1</sup>

3 <sup>1</sup>Department of Ecology, Faculty of Mathematics and Natural Sciences, University of Kassel,

4 Germany

5

6 \* Corresponding author

7 E-Mail: [a.ordynets@uni-kassel.de](mailto:a.ordynets@uni-kassel.de)

## 8 Abstract

9 Morphology of organisms is an important source of evidence for biodiversity assessment, taxonomic  
10 decisions, and understanding of evolution. Shape information about zoological and botanical objects  
11 is often treated quantitatively and in this form improves species identification. In studies of fungi,  
12 quantitative shape analysis was almost ignored. The disseminated propagules of fungi, the spores, are  
13 crucial for their taxonomy – currently in the form of linear measurements or subjectively defined  
14 shape categories. It remains unclear how much quantifying spore shape information can improve  
15 species identification. In this study, we tested the hypothesis that shape, as a richer source of  
16 information, overperforms size when performing automated identification of fungal species. We used  
17 the fungi of the genus *Subulicystidium* (Agaricomycetes, Basidiomycota) as a study object. We  
18 analysed 2D spore shape data via elliptic Fourier and Principal Component analyses. With flexible  
19 discriminant analysis, we achieved a slightly higher species identification success rate for shape  
20 predictors (61.5%) than for size predictors (59.1%). However, we achieved the highest rate for a  
21 combination of both (64.7%). We conclude that quantifying fungal spore shapes is worth the effort.  
22 We provide an open access protocol which, we hope, will stimulate a broader use of quantitative  
23 shape analysis in fungal taxonomy. We also discuss the challenges of such analyses that are specific to  
24 fungal spores.

25

## 26 Keywords

27 geometric morphometrics, classification, contour, fungi, outline, traditional morphometrics

## 28 Introduction

29 In eucaryotic organisms, morphology is an important source of evidence for biodiversity assessment,  
30 taxonomic decisions, and understanding of evolutionary and ecological processes. Morphological  
31 information is quickly accessible and can be processed at relatively low costs. Therefore it is broadly  
32 used by both researchers and citizen scientists. Morphological information, on the one hand, provides  
33 a starting point for molecular analyses, and on the other hand, serves as reference data to validate  
34 the molecular results [1].

35 Morphology covers two principal concepts: size and shape. The former is easier to measure and was  
36 dominating for more than a century in the quantitative analyses known as traditional morphometrics  
37 [2]. Although being important, the size alone is often insufficient for the delimitation of species or  
38 populations. For example, within a single taxonomic group of diatom algae (Bacillariophyceae), linear  
39 measurements allowed to delimit species in some genera [3] but not in others [4]. The authors of the  
40 latter study concluded that involving quantitative shape descriptors, in addition to size, would make  
41 delimitation of taxa more efficient. It is a discipline of geometric morphometrics that aims to quantify  
42 a shape, geometric information about the object that remains after removing the effects of location,  
43 rotation, and scale [5]. Tools of geometric morphometrics allow splitting the shape information into  
44 symmetric and asymmetric components and analyse them separately [6]. Besides dealing with richer  
45 data of numeric nature, geometric morphometric allows reconstruction of the original look of the  
46 object after analyses – a valuable property that traditional morphometrics does not offer [1,2].

47 Fungi are among the species-richest organism groups on Earth [7]. Generally, for morphology-based  
48 fungal taxonomy, the features of the disseminated propagules, the spores, are of the highest priority  
49 among phenotypic characters [8]. However, there is a difference in how the size and shape of spores  
50 are usually treated. The spore size is routinely used for species delimitations, mostly in the form of  
51 quantitative traits such as length and width [9,10]. Spore shape also plays a big role but has been  
52 treated differently. The length to width ratio is used frequently as a proxy of the spore shape [9].

53 However, it is based on linear measurements and has little use for reconstructing the full shape. In  
54 most cases, spore shape is treated as a qualitative trait. Spore shape terminology in mycology is a  
55 traditional system with dozens of terms that use common geometric shape categories (“globose”,  
56 “cylindric”) or similarity to some natural or cultural objects (“ovoid”, “filiform”). The picture  
57 becomes further complicated when subcategories are arbitrarily introduced, e.g. via adding prefix  
58 “sub-” or epithets “slightly” or “almost”. The subjectivity of this system represents a problem for  
59 reproducible research. Furthermore, such an approach makes impossible an assessment of the  
60 variation of a trait on an individual, populational, or species level. In their review, [1] concluded that  
61 “geometric morphometrics in the study of fungal shapes was far less employed compared to other  
62 microscopic organisms”.

63 To our knowledge, only two studies analysed the shape of fungal spores quantitatively. Study [11]  
64 found differences in the spore shape between the populations of one species and study [12] –  
65 between the populations as well as different species. However, neither of these mycological studies  
66 nor most other morphometric studies questioned in a quantitative way how the object’s shape  
67 performs compared to size when identifying species. An answer to this question would help to  
68 decide how much effort should be invested into digitizing shape information for such small objects  
69 as fungal spores. In this study, we test the hypothesis that shape, as a richer source of information,  
70 overperforms size when performing automated identification of fungal species. If it is the case,  
71 fungal spore shapes are worth the digitizing effort and integration into taxonomic workflows. To test  
72 this hypothesis, we are going to answer the following questions:

- 73 (i) Is it possible to adequately extract the shape information from images of fungal spores  
74 with the software that was developed for macroscopic objects?
- 75 (ii) Can the shape differences found in multivariate analyses be reconstituted as the  
76 outlines and recognized by a human eye?
- 77 (iii) Is it justified to split the spore shape information into symmetric and asymmetric  
78 portions or analysis of the overall shape variation would suffice?

79 As a test system for our study, we will use the genus *Subulicystidium* Parmasto (Hydnodontaceae,  
80 Trechisporales, Agaricomycetes, Basidiomycota, Fungi). It is a genus of fungi with 22 known species  
81 [13]. All known *Subulicystidium* species have smooth crust-shaped (corticioid) fruiting bodies and  
82 occur as saprotrophs on moderately or strongly decayed wood and are common in many forest  
83 ecosystems, especially tropical ones. For this genus, we own a large set of spore images after our  
84 previous study [14]. In that study, we performed traditional morphometric analysis of the spores  
85 while treating spore shapes only qualitatively. An additional advantage of our test system is the  
86 availability of DNA sequences for numerous specimens and the availability of the detailed genus-  
87 level phylogenetic tree. The DNA-based species assignments will serve as reference information to  
88 compare the performance of shape versus size data for automated species identification.

89

## 90 Methods

### 91 DNA data

92 We used a balanced set of 30 herbarium specimens which included ten species of *Subulicystidium*  
93 and where each species was equally represented by three specimens. We treated two clades of *S.*  
94 *perlongisporum* described in [15] as two separate species “*S. perlongisporum* 1” and “*S.*  
95 *perlongisporum* 2”. For all 30 specimens, we isolated and sequenced the internal transcribed spacer  
96 (ITS) of the nuclear ribosomal DNA as described in protocol 1 in [15] or used the sequences we  
97 produced earlier [14]. We processed raw sequence data with Geneious version 5.6.7 [16]. We  
98 imported the edited sequences to R version 4.0.3 [17] with the package “Biostrings” version 2.58.0  
99 [18] and performed the multiple sequence alignment with the package “msa” version 1.18.0 [19]  
100 using MUSCLE algorithm [20] and other settings as default. We then customly trimmed the ends of  
101 the alignment with the package “ips” version 0.0.11 [21] to the length when 15 of 30 sequences had  
102 non-ambiguous base characters in the first and last position of the alignment. The resulting

103 alignment had 734 nucleotide positions. We used the alignment viewer available in the package  
104 “ape” version 5.4.1 [22] to check visually the sequence alignment. According to the Akaike criterion  
105 [23], we identified “TrN+G+I” as the best-fitting nucleotide substitution model. We searched for the  
106 best-scoring maximum likelihood phylogenetic tree with the nearest neighbor interchange strategy  
107 and performed bootstrap analysis (1000 replicates) with the “phangorn” package version 2.5.5 [24].  
108 We visualized the result with the R package “ggtree” version 2.4.1 [25].

109 We submitted the newly generated DNA sequences to GenBank [26]. We provide the full list of the  
110 used DNA sequences with GenBank accessions and metadata on voucher specimens in supporting  
111 information S1.

112

### 113 Morphological data

#### 114 Spore terminology

115 To describe the spore morphology, we used the terms as they are found in [27] and [28]. The spores  
116 in *Subulicystidium*, as in all Basidiomycota, are produced externally on a sporangium called basidium  
117 and remain attached to it till they become mature and ready for discharge (Fig 1). It is the proximal  
118 part of the spore that directly contacts the basidium. The distal part of the spore is found on the  
119 opposite side of its long axis. The spore has an adaxial side, i.e. turned to the main axis of basidium,  
120 and opposite to it an abaxial side. On the proximal part of the spore, there is a projection called hilar  
121 appendix that is involved in the spore discharge from a basidium [27]. Observing hilar appendix on  
122 the adaxial side of the spore means the spore is seen in the lateral face. Observing hilar appendix  
123 directly on the main axis of the spore means the spore is seen in the frontal face. It is correct to  
124 compare the shapes of the spores within the same face. In our study, we focus on the spore’s lateral  
125 face which is more informative in the case of *Subulicystidium*.

126

127 **Fig 1. Crucial terms for describing a spore of the member of Agaricomycetes**

128

129 Image acquisition and pre-processing

130 We acquired and pre-processed images from light microscopy as described in detail in our online

131 protocol [29]. In this paper, we highlight the most essential steps and we illustrate a workflow of

132 image processing in Fig 2. We performed all work on images on a desktop computer with 64-bit

133 Windows 10 operating system (build 19041). We obtained images of spores from squash

134 preparations of fungal herbarium specimens examined at 1000× magnification (Fig 2A). The size of

135 the captured images (JPEG files) was 1024 × 768 or 2048 × 1536 pixels while the resolution was

136 always 96 dpi. We performed bulk image renaming with Bulk Rename Utility version 3.3.1.0 [30] and

137 conversion from JPEG to BMP graphic format with ImageMagick version 7.0.10- [31].

138

139 **Fig 2. Workflow showing the extraction of the shape and size information from a fungal spore.**

140 (A) Image capture and pre-processing, (B) Acquiring linear measurements (C) Acquiring chain codes

141 (D) Transforming chain codes to Normalized Elliptic Fourier Descriptors (E) Checking quality and

142 orientation of the outlines (F) Possibility to open and manage outline descriptors in a text editor. The

143 tools and programs used at each step are named on the left side of each colored panel.

144

145 For further processing, we selected those images that contained one or several healthy (not broken,

146 with intact cell wall) mature (not attached to basidia) and well-focused spores [29]. We selected also

147 only the spores that were laying clearly in the lateral face. Furthermore, for meaningful shape

148 analysis, spores had to be alignable, i.e. with hilar appendix stretching out to the same direction if

149 the spore were placed in the same orientation. Some images had to be mirrored to meet this

150 criterion. In some cases, we applied additional manual adjustments, namely painting white lines

151 around some parts of the spore outline, to enhance the clarity of spore outlines and to ensure the

152 absence of contact with the structures that are other spores or not spores (crystals or hyphae),  
153 similar to [10] and [32]. These adjustments did not affect the geometric properties of the spore  
154 outlines but enabled a correct outline extraction. Raw and pre-processed images and all information  
155 extracted from them are available as a published dataset [33].

156

## 157 Processing shape information

158 Fungal spores are practically devoid of landmarks, i.e. distinct points that mark angles or cavities and  
159 can be unambiguously assigned to an object. Therefore, for fungal spores, methods aiming to  
160 reconstruct the complete outline are advantageous. Among such methods, Elliptic Fourier analysis  
161 [34] is most commonly employed. It uses an ellipse as a starting shape and searches for the  
162 coefficient values that transform the ellipse into the shape that reproduces the original outline of  
163 the object. These coefficients are called Elliptic Fourier Descriptors. After normalization, i.e.  
164 removing the effects of size, rotation, shift, and starting point of outline recording, they are called  
165 Normalized Elliptic Fourier Descriptors (NEFDs) and are used in statistical analysis as variables  
166 describing the shape [1].

167 We performed Elliptic Fourier analysis in the software package SHAPE version 1.3 [35]  
168 (<http://lbm.ab.a.u-tokyo.ac.jp/~iwata/shape/>). We used consequently each of the following  
169 programs from this package for different analysis steps: ChainCoder, Ch2Nef, NefViewer, PrinComp,  
170 and PrinPrint [29]. We started with grayscaling the BMP images in the program ChainCoder (Fig 2C).  
171 Then we converted the images to binary (assigning white pixels to spores and black to background)  
172 based on a threshold that was mostly automatically selected by ChainCoder and was only rarely  
173 adjusted manually. To remove the shape artifacts, we applied an erosion-dilation filter (that excludes  
174 the noisy pixels from the outline) and rarely also a dilation-erosion filter (to fill in artifact cavities).  
175 Then a chain code, i.e. a sequence of x and y coordinates describing the outline, was taken for each  
176 spore.



177 We imported the chain codes to Ch2Nef program [35] and checked the orientation of all spores to  
178 be the same, i.e. spore hilar appendix placed in the upper left quarter of the image (Fig 2D). When  
179 necessary, we applied 180-degree rotation to some of the spores. Ch2Nef then transformed the  
180 chain code into the Normalized Elliptic Fourier Descriptors (NEFDs). As a depth of detailisation of the  
181 contour information, we opted for 20 levels that are called harmonics in the elliptic Fourier analysis  
182 [34]. In general, other studies of organism shapes used from 15 to 30 harmonics [36,37], and using  
183 20 harmonics was sufficient in the classical study from authors of the SHAPE package [6,35]. As each  
184 harmonic is described by four coefficients (= Elliptic Fourier Descriptors), there were 80 coefficients  
185 that characterised the shape of each spore. As the first three coefficients are always constant, there  
186 were 77 coefficients serving as shape variables for the next analysis step. To normalize the Elliptic  
187 Fourier Descriptors, we used the approach based on the first harmonic [35]. We checked that NEFDs  
188 are alignable with the NefViewer program (Fig 2E).

189 We combined manually NEFDs for individual specimens into a single .txt file (Fig 2F). To reduce the  
190 multidimensionality of NEFDs data, we run on it the Principal Component Analysis (PCA) in PrinComp  
191 program [35]. We used the flexibility of PrinComp and performed in total three principal component  
192 analyses (PCAs): i) considering only the symmetric shape variation, ii) considering only the  
193 asymmetric shape variation, and iii) considering overall shape variation not differentiated into  
194 symmetric and asymmetric (hereinafter called global shape variation). As a result of each PCA, we  
195 retained those principal components (PC) that explained a substantial amount of variation and were  
196 marked by PrinComp as having an eigenvalue >1. Such PCs were called “effective” in PrinComp. We  
197 inspected visually the shape variation accounted for by each effective PC with PrinPrint program  
198 [29]. The latter reconstructed the mean shape and plus and minus two times the standard deviation  
199 shape for each principal component [35].

200

## 201 Processing size information

202 For exactly those spores for which NEFDs were obtained, we took also the linear measurement:  
203 length (the longest dimension) and width (the broadest dimension) according to the standard  
204 accepted in mycology [9]. We used Fiji distribution of ImageJ version 1.53c [38] as shown in Fig 2B  
205 and described in [29]. Fiji does not differentiate whether the measurement is of a category “length”  
206 or “width”. Therefore, we measured constantly firstly length and then width or each spore. Though  
207 these values were originally placed in a single column, we split them into length and width columns  
208 in R using our protocol [29]. Based on length and width values, we also derived their ratio and used it  
209 as an additional variable in statistical analyses.

210

## 211 Comparative analyses

212 While obtaining the shape descriptors and linear measurements, we had control of the number of  
213 spores used per specimen and image. However, if the image contained several spores, we were not  
214 able to align the shape descriptors with linear measurements for each particular spore. Even though  
215 the input was the same .bmp image, the software for obtaining the shape data (SHAPE) and size data  
216 (Fiji) named individual measurements slightly differently. We could overcome it only by producing  
217 average-per-image trait values and using them as observations in correlations and discriminant  
218 analysis [29]. To produce average-per-image trait values, we used regular expressions in R as well as  
219 packages “stringr” version 1.4.0 [39] and “dplyr” version 1.3.0 [40].

220 For comparison, we assigned the morphometric traits to one of the five categories:

- 221 i) principal components of symmetric shape variation
- 222 ii) principal components of asymmetric shape variation
- 223 iii) principal components of global shape variation
- 224 iv) linear measurements (length and width)

225 v) length to width ratio

226 We explored how similar were all morphometric traits between themselves by Spearman  
227 correlations. To answer which morphometric traits allow more efficient automated identification of  
228 fungal species, we applied discriminant analysis. We assessed how accurate the individual traits and  
229 their combinations can identify (classify) to species level the observations whose species identity is  
230 not known to the statistical model. We found that trait values within species are not necessarily  
231 normally distributed and between the species do not have equal variance. For details, see  
232 supporting information S2 with the results of Shapiro-Wilk tests (made with R package  
233 “RVAideMemoire” version 0.9-79, [41]) and Levene tests (made with R package “heplots” version  
234 1.3-8 [42]). Therefore, we applied an appropriate for such cases flexible discriminant analysis [43]  
235 implemented in “mda” R package version 05-2 [44]. We were randomly subsetting the data into the  
236 train (70%) and test (30%) portions attempting to balance the presence of data for different species  
237 with R package “caret” version 6.0-86 [45]. We repeated to subset the data into train and test  
238 portions 1000 times and then calculated the average identification (i.e. correct species assignment)  
239 success rate across subsettings using the R code adjusted from [46].

240 We managed data in R with the packages “here” version 1.0.1 [47], “conflicted” version 1.0.4 [48],  
241 “readr” version 1.4.0 [49], “data.table” version 1.13.4 [50], “dplyr” version 1.3.0 [40], and “report”  
242 version 0.2.0 [51]. We visualized the results with the packages „ggplot2“ version 3.3.3 [52], “ggpubr”  
243 version 0.4.0 [53], function “cor.mtest” [54] and package “corrplot” version 0.84 [55]. We edited Figs  
244 1 and 4 with Inkscape version 0.92.5 [56] and Fig 2 also with Miro online whiteboard  
245 (<https://miro.com/>). We provide the R project with the code, input data and results of analyses in  
246 supporting information S2 and as a repository on GitHub  
247 ([https://github.com/ordynets/size\\_vs\\_shape](https://github.com/ordynets/size_vs_shape)).

248

## 249 Results

250 Maximum likelihood phylogenetic analysis showed all ten *Subulicystidium* species on the  
251 phylogenetic tree as clearly separate clades, mostly with high bootstrap supports (Fig 3).

252

### 253 **Fig 3. Phylogenetic relationship of 10 *Subulicystidium* species treated in this study**

254

255 After all quality filtering steps, we were able to analyse between 10 and 37 spores per specimen  
256 which totaled 511 spores from 30 specimens. These spores were captured in 401 images and each  
257 image contained one to four spores (supporting information S2). Therefore we considered 401  
258 average-per-image values as observations for analyses.

259 PCA of symmetric shape variation identified only the first axis as effective (capturing 98,7% of the  
260 variation in data) while PCA of asymmetric variation three first axes (capturing 83.03, 6.63 and 4.11%  
261 of variation), and PCA of global variation two axes (capturing 94.57 and 2.91% of variation). Together  
262 with the spore length, spore width, and length to width ratio, this summed up to nine traits which  
263 we compared in terms of efficiency for automated species identification (supporting information S2).

264 By inspecting visually the shape variation accounted for by each principal component we found that  
265 the 1<sup>st</sup> PC of symmetric variation reflected well the relative thickness of spores (Fig 4). The 1<sup>st</sup> PC of  
266 asymmetric shape variation reflected the direction of single curving of the long axis of the spore. The  
267 2<sup>nd</sup> and 3<sup>rd</sup> PCs of asymmetric shape variation reflected the variation in curvature of the proximal  
268 and distal end of the spore, respectively. The effects of the 1<sup>st</sup> and 2<sup>nd</sup> PCs of the global shape  
269 variation corresponded to the 1<sup>st</sup> PC of symmetric and 1<sup>st</sup> PC of asymmetric shape variation,  
270 respectively.

271

### 272 **Fig 4. Ranges of shape variation that separate principal components account for.**

273

274 When correlating the individual trait variables, we found that 1<sup>st</sup> PCs of symmetric, asymmetric, and  
275 global shape variation correlated strongly positively with each other (Fig 5). All they correlated  
276 strongly negatively with the length and moderately positively with the width of the spores. The 2<sup>nd</sup>  
277 PC of asymmetric shape variation correlated moderately negatively with the spore width while the  
278 3<sup>rd</sup> PC of asymmetric shape variation and 2<sup>nd</sup> PC of the global shape variation did not correlate  
279 significantly with any other trait. Length and width correlated moderately negatively between  
280 themselves and each correlated very differently with the length to width ratio, though the  
281 correlation was stronger between the length and length to width ratio.

282

283 **Fig 5. Spearman correlations of spore traits.**

284 Colors show the direction of correlation and highlight only significant correlation values (at level  
285  $p=0.05$ )

286

287 In the discriminant analysis, the species identification success rate for the individual trait group was  
288 highest for the global shape variation (61.5%, Fig 6) while was slightly lower for length and width  
289 (59.1%). Symmetric shape variation identified the fungal species better than the length to width  
290 ratio (57.9% vs. 53.8%). The asymmetric shape variation had the lowest identification success rate,  
291 viz. 46.9%. When combining the traits of different groups, the highest identification success rate was  
292 achieved for the combination of symmetric, asymmetric shape variation and linear measurements  
293 (64.7%). By using the global shape variation instead of separate symmetric and asymmetric, the  
294 success rate was slightly lower (62.4%).

295

296 **Fig 6. Species identification success rates in discriminant analysis for separate spore traits and**  
297 **their combinations.**

298 Abbreviations on y axis: S = symmetric shape variation (first principal component), A = asymmetric  
299 shape variation (three first principal components), G = global shape variation (two first principal  
300 components), LW = length + width, Q = length to width ratio, QLW = length to width ratio + length +  
301 width, GLW = global shape variation + length + width, SALW = symmetric shape variation +  
302 asymmetric shape variation + length + width.

303

304

305 Discussion

306 Quantitative analysis of shapes helps to better identify and describe the organisms. In studies of  
307 fungi, despite their immense morphological diversity, quantitative shape analysis was almost  
308 ignored. In this study, we confirmed the hypothesis that shape, as a richer source of information,  
309 outperforms size during automated identification of fungal species by their spores. The highest  
310 identification success rate was achieved in a discriminant model that combined shape and size  
311 descriptors. The symmetric shape variation outperformed the classical length to width ratio. In  
312 general, we found that

- 313 (i) It is possible to adequately extract the shape information from microscopy images of  
314 fungal spores;
- 315 (ii) It is possible to recognise by a human eye the spore shape differences reconstituted  
316 after the multivariate analyses;
- 317 (iii) It is justified to split the spore shape information into symmetric and asymmetric  
318 portions for separate analyses.

319 As quantitative shape analysis has been barely applied in mycology, we first had to ensure that  
320 available tools for extracting shape information can be used for our goal. Many of the tools were  
321 developed to work on the high-quality images of macroscopic organisms, often photographed as a  
322 single object per image in the desired orientation [57–59]. We opted for the program package  
323 SHAPE [35] which allows extracting several outlines from the same image, has flexibility for  
324 performing PCA and in general, has a convenient interface and detailed manual. Despite this  
325 package was originally designed for images of macroscopic objects, we successfully applied it to the  
326 outline extraction from the images with a modest resolution made by our microscope camera. The  
327 disadvantage of using SHAPE is a need to switch between the separate programs, meaning handling  
328 several outcomes and an extra effort in data management. Furthermore, the graphical user interface  
329 of SHAPE (or any other GUI program) means investing massive time effort when repeating the  
330 analysis and increased risk of producing an error. Therefore, in the future, it is advisory to work in a  
331 single environment with all analysis steps written as a code. This will simplify the data management  
332 and enhance the reproducibility of the analyses. Functions in R language designed by [60] and  
333 further developed by [61] and [62] are promising for this.

334 With our study design, we observed high correlations between several trait variables. The most  
335 important to note is the correlation between the shape descriptors (PC1 of symmetric and  
336 asymmetric variation) and size descriptors (especially length). This is due to our choice to represent  
337 the size as linear measurements, which are known to be geometrically dependent on a shape [2].  
338 We kept linear measurements as size descriptors to demonstrate their properties and to explore the  
339 performance of these classical variables for species identification. We also generated the size  
340 variable that is a combination of separate linear measurements and is less independent of shape  
341 (square root of the product of length time width, as one possible option according to Claude 2008).  
342 This size variable indeed correlated less with shape variables but in discriminant model predicted the  
343 species much poorer than the length and width together (38.9% vs 59.1%, see supplementary  
344 information S2). In geometric morphometrics, there are also other measures of the size that are

345 independent of shape and are worth the look by fungal taxonomists [60,63]. Among other trait  
346 variables, the correlation between PC1 of global and symmetric shape variation, PC1 of global and  
347 asymmetric shape variation, and length and length to width ratio are easily explained by their nested  
348 nature. Therefore we did not add these highly correlating variable pairs to the same discriminant  
349 models. On the other hand, we struggled to explain the rather high correlation between PC1 of  
350 symmetric and asymmetric shape variation. We guess that it is due to a strongly dominating  
351 character of PC1 of symmetric shape variation, which was constructed with an account of the first-  
352 level elliptic Fourier harmonic (D1).

353 The identification success rate in our discriminant analyses reached the maximum value of 64.69%. It  
354 is hard to compare our results with other studies where authors used different traits and/or  
355 different classification methods. Benyon et al. (1999) achieved an identification success rate of  
356 66.2% using seven traits and a higher rate (74.4%) using 20 traits of fungal spores (mostly size  
357 descriptors). Authors of [4] obtained similar to our results in discriminant analyses of size and  
358 texture traits in diatom algae (55.1% correctly identified items). Authors of [65] reached 100% or  
359 nearly such rates for species of diatom algae by shape and texture descriptors. However, they used  
360 discriminant analysis as a dimensionality reduction tool and above its result applied other  
361 classification techniques. Authors of [66] evaluated their analyses of diatom cell shapes visually, i.e.  
362 as strength of separation of observations in the space of discriminant functions. They concluded that  
363 taxa with distinct shapes were separated well while the taxa with similar shapes were separated to a  
364 less extent. The identification success rates in [32] for statoliths in cubomedusae were comparable,  
365 after cross-validation, with ours, but were highly dependent on the number of observations per  
366 group. Due to technical reasons explained in Methods section, we performed analyses on average-  
367 per-image data. We admit that working with spore-level data would provide a more precise estimate  
368 of the correct identification rate.



369 Future work on quantitative shape analysis of fungal spores should cope with several challenges.  
370 Fungal spores may have very different outline properties in lateral versus frontal face. In the current  
371 study, we focused on the lateral face which is more peculiar in *Subulicystidium* and allows to capture  
372 the curvature along the spores' long axis (while the frontal face masks this feature). However, in  
373 other fungal taxa, the lateral and frontal faces are both important [28] and their shapes should be  
374 analysed with the same attention. Authors of [32] combined three faces of the objects to achieve a  
375 high identification success rate. In fungi, it may be easy to identify the spore as exposed in the lateral  
376 face if its hilar appendix is large enough. Unfortunately, this is not the case for all species. Special  
377 care should be taken to identify the position of the hilar appendix in the needle-like spores (as in *S.*  
378 *cochleum* and *S. perlongisporum* in our dataset). Applying scanning electron microscopy may help to  
379 identify correctly the hilar appendix but also to get a detailed picture of the surface of the fungal  
380 spore. While our study focused on the fungi with smooth spores, the latter in many taxa bear  
381 additional projections like warts or ridges or distinct spines. These elements would be difficult to  
382 capture with the elliptic Fourier descriptors because of the mathematical properties of the method  
383 [1]. Therefore, ornamented spores of fungi give a chance to bring another approach, landmark-  
384 based methods of geometric morphometric, to mycology. These can be implemented in a two-  
385 dimensional and even three-dimensional space. Finally, different properties of the spores in lateral  
386 versus frontal face, as well as the availability of the several spore types per species in many fungal  
387 lineages, offer a possibility to bring the machine learning techniques to mycology.

388 We conclude that quantifying fungal spore shapes is worth the effort. We provide an open access  
389 protocol to propagate a broader use of quantitative shape analysis in fungal taxonomy and to  
390 stimulate the development of more efficient solutions to address the challenges we discussed above.

391

## 392 Data Availability

393 Metadata on studied voucher specimens is provided in supporting information S1. DNA sequences  
394 newly generated for this study are available from GenBank as accessions [MW711723-MW711729](#).  
395 Raw and pre-processed images and all information extracted from them are available as a published  
396 dataset (Ordynets et al. 2021b, <https://doi.org/10.15156/BIO/807451>). The R project with the code,  
397 input data, and results of analyses is provided in supporting information S2 and as a repository on  
398 GitHub ([https://github.com/ordynets/size\\_vs\\_shape](https://github.com/ordynets/size_vs_shape)).

399

## 400 Acknowledgements

401 We acknowledge the curators of fungal collections in ARAN, CWU, GB, LY, and O for providing  
402 specimens for our study, and personally Karl-Henrik Larsson, Janett Riebesehl, and Manuel Striegel  
403 who collected most of the specimens. David Scherf, Ludmila Lysenko, Ilka Kellner, Robert Liebisch,  
404 and Jonathan Denecke performed the DNA lab work and helped with the microscopy of the  
405 collections. Anton Savchenko, Oleh Prylutskyi, and Iryna Yatsiuk provided feedback on the earlier  
406 version of the protocol for extracting the shape and size information from the spores.

407

## 408 References

- 409 1. Fodor E, Hâruța OI. Geometric Morphometrics and the Shape of Microscopic Organisms.  
410 Modern Trends in Diatom Identification. 2020; 197–217. doi:10.1007/978-3-030-39212-3\_12
- 411 2. Zelditch M, Swiderski DL, Sheets HD. Geometric morphometrics for biologists: a primer. Second  
412 edition. Amsterdam: Elsevier/Academic Press; 2012.
- 413 3. Paull TM, Hamilton PB, Gajewski K, LeBlanc M. Numerical analysis of small Arctic diatoms  
414 (Bacillariophyceae) representing the *Staurosira* and *Staurosirella* species complexes.  
415 *Phycologia*. 2008;47: 213–224. doi:10.2216/07-17.1
- 416 4. Blanco S, Borrego-Ramos M, Olenici A. Disentangling diatom species complexes: does  
417 morphometry suffice? *PeerJ*. 2017;5: e4159. doi:10.7717/peerj.4159

- 418 5. Kendall DG. The Diffusion of Shape. *Advances in Applied Probability*. 1977;9: 428–430.  
419 doi:10.2307/1426091
- 420 6. Iwata H, Niikura S, Matsuura S, Takano Y, Ukai Y. Evaluation of variation of root shape of  
421 Japanese radish (*Raphanus sativus* L.) based on image analysis using elliptic Fourier descriptors.  
422 *Euphytica*. 1998;102: 143–149. doi:10.1023/A:1018392531226
- 423 7. Mora C, Tittensor DP, Adl S, Simpson AGB, Worm B. How Many Species Are There on Earth and  
424 in the Ocean? Mace GM, editor. *PLoS Biology*. 2011;9: e1001127.  
425 doi:10.1371/journal.pbio.1001127
- 426 8. Sieber TN, Petrini O, Greenacre MJ. Correspondence Analysis as a Tool in Fungal Taxonomy.  
427 *Systematic and Applied Microbiology*. 1998;21: 433–441. doi:10.1016/S0723-2020(98)80053-2
- 428 9. Parmasto E, Parmasto I, Möls T. Variation of basidiospores in the hymenomycetes and its  
429 significance to their taxonomy. Bresinsky A, Butin H, Schwantes HO, editors. Berlin, Stuttgart: J.  
430 Cramer; 1987.
- 431 10. Anikster Y, Eilam T, Bushnell WR, Kosman E. Spore dimensions of *Puccinia* species of cereal  
432 hosts as determined by image analysis. *Mycologia*. 2005;97: 474–484.  
433 doi:10.1080/15572536.2006.11832823
- 434 11. Infantino A, Zaccardelli M, Costa C, Ozkilinc H, Habibi A, Peever T. A new disease of grasspea  
435 (*Lathyrus sativus*) caused by *Ascochyta lentis* var. *lathyri*. *Journal of Plant Pathology*. 2016;98:  
436 541–548. doi:10.4454/JPP.V98I3.008
- 437 12. Fodor E, Hâruța O, Milenković I, Lyubenova A, Tziros G, Keča N, et al. Geometric morphometry  
438 of *Phytophthora plurivora* sporangia. *Annals of Forest Research*. 2015;58: 275-294–294.  
439 doi:10.15287/afr.2015.411
- 440 13. Index Fungorum. Index Fungorum. 2021. Available: <http://www.indexfungorum.org>
- 441 14. Ordynets A, Scherf D, Pansegrau F, Denecke J, Lysenko L, Larsson K-H, et al. Short-spored  
442 *Subulicystidium* (Trechisporales, Basidiomycota): high morphological diversity and only partly  
443 clear species boundaries. *Mycology*. 2018;35: 41–99. doi:10.3897/mycokeys.35.25678
- 444 15. Ordynets A, Liebisch R, Lysenko L, Scherf D, Volobuev S, Saitta A, et al. Morphologically similar  
445 but not closely related: the long-spored species of *Subulicystidium* (Trechisporales,  
446 Basidiomycota). *Mycological Progress*. 2020;19: 691–703. doi:10.1007/s11557-020-01587-3
- 447 16. Kearse M, Moir R, Wilson A, Stones-Havas S, Cheung M, Sturrock S, et al. Geneious Basic: an  
448 integrated and extendable desktop software platform for the organization and analysis of  
449 sequence data. *Bioinformatics*. 2012;28: 1647–1649. doi:10.1093/bioinformatics/bts199
- 450 17. R Core Team. R: A Language and Environment for Statistical Computing. Vienna, Austria: R  
451 Foundation for Statistical Computing; 2020. Available: <https://www.r-project.org/>
- 452 18. Pagès H, Aboyoun P, Gentleman R, DebRoy S. Biostrings: Efficient manipulation of biological  
453 strings. 2019. Available: <https://bioconductor.org/packages/Biostrings>
- 454 19. Bodenhofer U, Bonatesta E, Horejš-Kainrath C, Hochreiter S. msa: an R package for multiple  
455 sequence alignment. *Bioinformatics*. 2015;31: 3997–3999. doi:10.1093/bioinformatics/btv494

- 456 20. Edgar RC. MUSCLE: multiple sequence alignment with high accuracy and high throughput.  
457 Nucleic Acids Research. 2004;32: 1792–1797. doi:10.1093/nar/gkh340
- 458 21. Heibl C, Cusimano N, Krah F-S. ips: Interfaces to Phylogenetic Software in R. 2019. Available:  
459 <https://CRAN.R-project.org/package=ips>
- 460 22. Paradis E, Schliep K. ape 5.0: an environment for modern phylogenetics and evolutionary  
461 analyses in R. Bioinformatics. 2019;35: 526–528. doi:10.1093/bioinformatics/bty633
- 462 23. Akaike H. Information theory and an extension of the maximum likelihood principle. In: Petrov  
463 B, Csaki B, editors. Second International Symposium on Information Theory. Budapest:  
464 Academiai Kiado; 1973. pp. 267–281.
- 465 24. Schliep KP. phangorn: phylogenetic analysis in R. Bioinformatics. 2011;27: 592–593.  
466 doi:10.1093/bioinformatics/btq706
- 467 25. Yu G, Smith DK, Zhu H, Guan Y, Lam TT. ggtree: an R package for visualization and annotation of  
468 phylogenetic trees with their covariates and other associated data. Methods in Ecology and  
469 Evolution. 2017;8: 28–36. doi:10.1111/2041-210X.12628
- 470 26. Benson DA, Cavanaugh M, Clark K, Karsch-Mizrachi I, Lipman DJ, Ostell J, et al. GenBank.  
471 Nucleic Acids Res. 2013;41: D36–42. doi:10.1093/nar/gks1195
- 472 27. Ingold CT, Hudson HJ. Basidiomycotina. In: Ingold CT, Hudson HJ, editors. The Biology of Fungi.  
473 Dordrecht: Springer Netherlands; 1993. pp. 75–108. doi:10.1007/978-94-011-1496-7\_5
- 474 28. Kõljalg U. Tomentella (Basidiomycota) and related genera in temperate Eurasia. Oslo:  
475 Fungiflora; 1996.
- 476 29. Ordynets A, Keßler S, Willemsens C. Extracting shape and size information from fungal spores.  
477 protocols.io. 2021. doi:dx.doi.org/10.17504/protocols.io.bdeii3ce
- 478 30. TGRMN Software Company. Bulk Rename Utility. TGRMN Software Company; 2019. Available:  
479 <https://www.bulkrenameutility.co.uk/>
- 480 31. The ImageMagick Development Team. ImageMagick. 2021. Available: <https://imagemagick.org>
- 481 32. Mooney CJ, Kingsford MJ. Statolith Morphometrics Can Discriminate among Taxa of Cubozoan  
482 Jellyfishes. PLOS ONE. 2016;11: e0155719. doi:10.1371/journal.pone.0155719
- 483 33. Ordynets A, Lysenko L, Kellner I, Scherf D, Liebisch R, Denecke J, et al. Data for the study  
484 “Quantitative analysis of spore shapes improves identification of fungi.” Universität  
485 Gesamthochschule Kassel; 2021. doi:10.15156/BIO/807451
- 486 34. Kuhl FP, Giardina CR. Elliptic Fourier features of a closed contour. Computer Graphics and  
487 Image Processing. 1982;18: 236–258. doi:10.1016/0146-664X(82)90034-X
- 488 35. Iwata H, Ukai Y. SHAPE: A Computer Program Package for Quantitative Evaluation of Biological  
489 Shapes Based on Elliptic Fourier Descriptors. Journal of Heredity. 2002;93: 384–385.  
490 doi:10.1093/jhered/93.5.384
- 491 36. Rohlf FJ, Archie JW. A Comparison of Fourier Methods for the Description of Wing Shape in  
492 Mosquitoes (Diptera: Culicidae). Syst Biol. 1984;33: 302–317. doi:10.2307/2413076

- 493 37. Yang H-P, Ma C-S, Wen H, Zhan Q-B, Wang X-L. A tool for developing an automatic insect  
494 identification system based on wing outlines. *Sci Rep.* 2015;5: 1–11. doi:10.1038/srep12786
- 495 38. Schindelin J, Arganda-Carreras I, Frise E, Kaynig V, Longair M, Pietzsch T, et al. Fiji: an open-  
496 source platform for biological-image analysis. *Nature Methods.* 2012;9: 676–682.  
497 doi:10.1038/nmeth.2019
- 498 39. Wickham H. *stringr: Simple, Consistent Wrappers for Common String Operations.* 2019.  
499 Available: <https://CRAN.R-project.org/package=stringr>
- 500 40. Wickham H, François R, Henry L, Müller K. *dplyr: A Grammar of Data Manipulation.* 2021.  
501 Available: <https://CRAN.R-project.org/package=dplyr>
- 502 41. Hervé M. *RVAideMemoire: Testing and Plotting Procedures for Biostatistics.* 2021. Available:  
503 <https://CRAN.R-project.org/package=RVAideMemoire>
- 504 42. Fox J, Friendly M, Monette G. *heplots: Visualizing Tests in Multivariate Linear Models.* 2021.  
505 Available: <https://CRAN.R-project.org/package=heplots>
- 506 43. Hastie T, Tibshirani R, Buja A. Flexible Discriminant Analysis by Optimal Scoring. *Journal of the*  
507 *American Statistical Association.* 1994;89: 1255–1270. doi:10.1080/01621459.1994.10476866
- 508 44. Hastie T, Tibshirani R, Leisch F, Hornik K, Ripley BD, Narasimhan B. *mda: Mixture and Flexible*  
509 *Discriminant Analysis.* 2020. Available: <https://CRAN.R-project.org/package=mda>
- 510 45. Kuhn M, Wing J, Weston S, Williams A, Keefer C, Engelhardt A, et al. *caret: Classification and*  
511 *Regression Training.* 2020. Available: <https://CRAN.R-project.org/package=caret>
- 512 46. Martos G. *Discriminant Analysis in R.* 2020 [cited 6 Nov 2020]. Available: [https://rstudio-pubs-](https://rstudio-pubs-static.s3.amazonaws.com/35817_2552e05f1d4e4db8ba87b334101a43da.html)  
513 [static.s3.amazonaws.com/35817\\_2552e05f1d4e4db8ba87b334101a43da.html](https://rstudio-pubs-static.s3.amazonaws.com/35817_2552e05f1d4e4db8ba87b334101a43da.html)
- 514 47. Müller K. *here: A Simpler Way to Find Your Files.* 2020. Available: [https://CRAN.R-](https://CRAN.R-project.org/package=here)  
515 [project.org/package=here](https://CRAN.R-project.org/package=here)
- 516 48. Wickham H. *conflicted: An Alternative Conflict Resolution Strategy.* 2019. Available:  
517 <https://CRAN.R-project.org/package=conflicted>
- 518 49. Wickham H, Hester J. *readr: Read Rectangular Text Data.* 2020. Available: [https://CRAN.R-](https://CRAN.R-project.org/package=readr)  
519 [project.org/package=readr](https://CRAN.R-project.org/package=readr)
- 520 50. Dowle M, Srinivasan A. *data.table: Extension of `data.frame`.* 2020. Available: [https://CRAN.R-](https://CRAN.R-project.org/package=data.table)  
521 [project.org/package=data.table](https://CRAN.R-project.org/package=data.table)
- 522 51. Makowski D, Ben-Shachar MS, Patil I, Lüdtke D. Automated reporting as a practical tool to  
523 improve reproducibility and methodological best practices adoption. CRAN. 2020. Available:  
524 <https://github.com/easystats/report>
- 525 52. Wickham H. *ggplot2: elegant graphics for data analysis.* New York: Springer; 2016. Available:  
526 <https://ggplot2.tidyverse.org>
- 527 53. Kassambara A. *ggpubr: “ggplot2” Based Publication Ready Plots.* 2020. Available:  
528 <https://CRAN.R-project.org/package=ggpubr>

- 529 54. Anonym. Visualize correlation matrix using correlogram - Easy Guides - Wiki - STHDA. 2020  
530 [cited 6 Nov 2020]. Available: <http://www.sthda.com/english/wiki/visualize-correlation-matrix->  
531 [using-correlogram](http://www.sthda.com/english/wiki/visualize-correlation-matrix-using-correlogram)
- 532 55. Wei T, Simko V. R package “corrplot”: Visualization of a Correlation Matrix. 2017. Available:  
533 <https://github.com/taiyun/corrplot>
- 534 56. Inkscape Project. Inkscape. 2020. Available: <https://inkscape.org>
- 535 57. Libungan LA, Pálsson S. ShapeR: An R package to study otolith shape variation among fish  
536 populations. PLoS ONE. 2015;10. doi:10.1371/journal.pone.0121102
- 537 58. Rohlf FJ. The tps series of software. *Hystrix It J Mamm*. 2015;26: 9–12. doi:10.4404/hystrix-  
538 26.1-11264
- 539 59. Chuanromanee TS, Cohen JI, Ryan GL. Morphological Analysis of Size and Shape (MASS): An  
540 integrative software program for morphometric analyses of leaves. *Applications in Plant*  
541 *Sciences*. 2019;7: e11288. doi:10.1002/aps3.11288
- 542 60. Claude J. *Morphometrics with R*. New York, NY: Springer New York; 2008. doi:10.1007/978-0-  
543 387-77789-4
- 544 61. Bonhomme V, Picq S, Gaucherel C, Claude J. Momocs: outline analysis using R. *Journal of*  
545 *Statistical Software*. 2014;56. doi:10.18637/jss.v056.i13
- 546 62. Stela B, Monleón Getino T. Facilitating the automatic characterisation, classification and  
547 description of biological images with the VisionBioShape package for R. *Open Access Library*  
548 *Journal*. 2016;3. doi:10.4236/oalib.1103108
- 549 63. Rohlf FJ. *Morphometrics*. *Annual Review of Ecology and Systematics*. 1990;21: 299–316.
- 550 64. Benyon FHL, Jones AS, Tovey ER, Stone G. Differentiation of allergenic fungal spores by image  
551 analysis, with application to aerobiological counts. *Aerobiologia*. 1999;15: 211–223.  
552 doi:10.1023/A:1007501401024
- 553 65. Sánchez C, Cristóbal G, Bueno G. Diatom identification including life cycle stages through  
554 morphological and texture descriptors. *PeerJ*. 2019;7. doi:10.7717/peerj.6770
- 555 66. Wishkerman A, Hamilton PB. Shape outline extraction software (DiaOutline) for elliptic Fourier  
556 analysis application in morphometric studies. *Applications in Plant Sciences*. 2018;6.  
557 doi:10.1002/aps3.1204

558

## 559 [Supporting information](#)

560 S1 Table. GenBank accessions of used DNA sequences and metadata on voucher specimens

561 S2 Appendix. R project with the code, input data, and results of analyses.

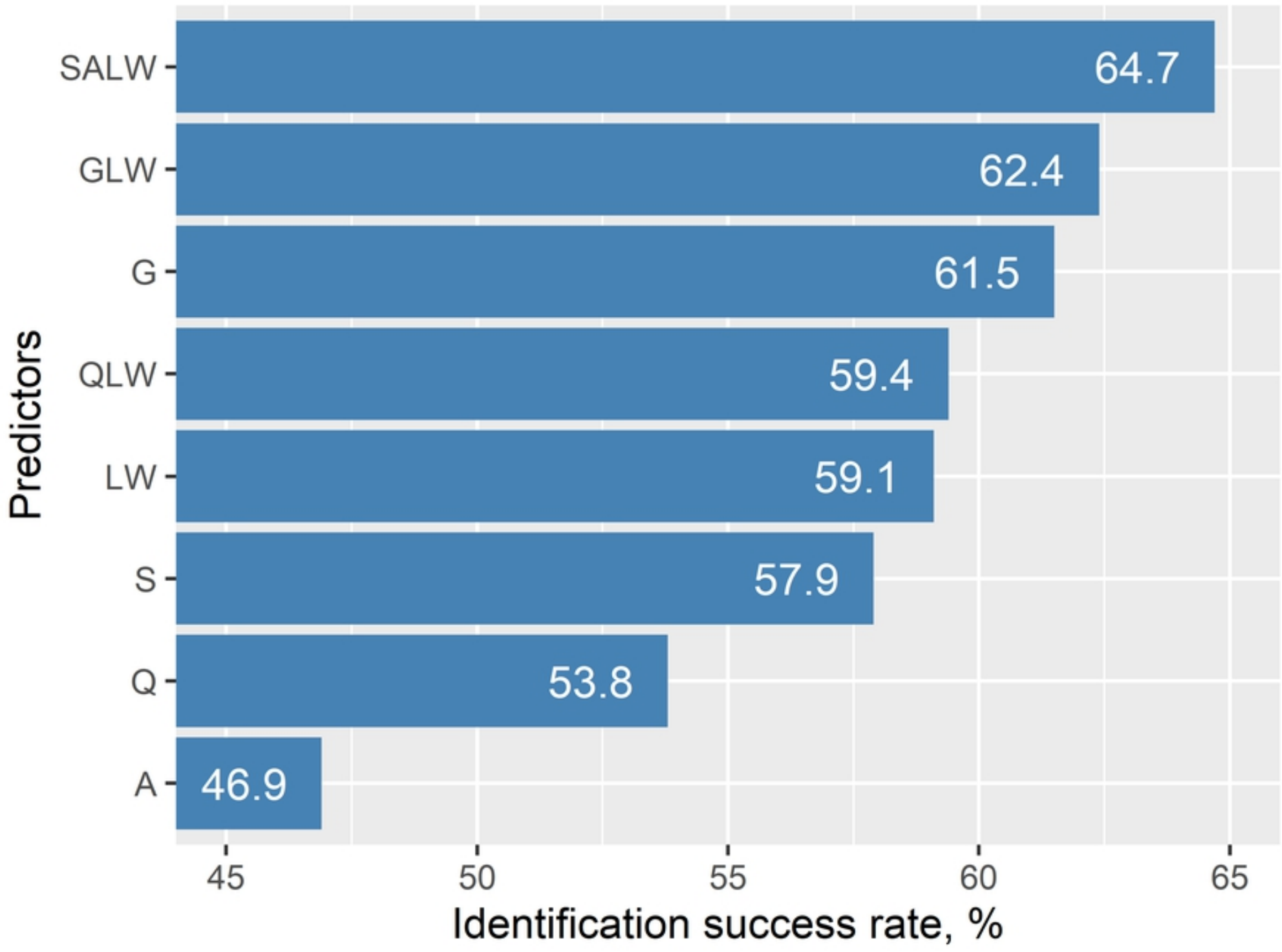


Fig 6

Spore in lateral face

Spore in frontal face

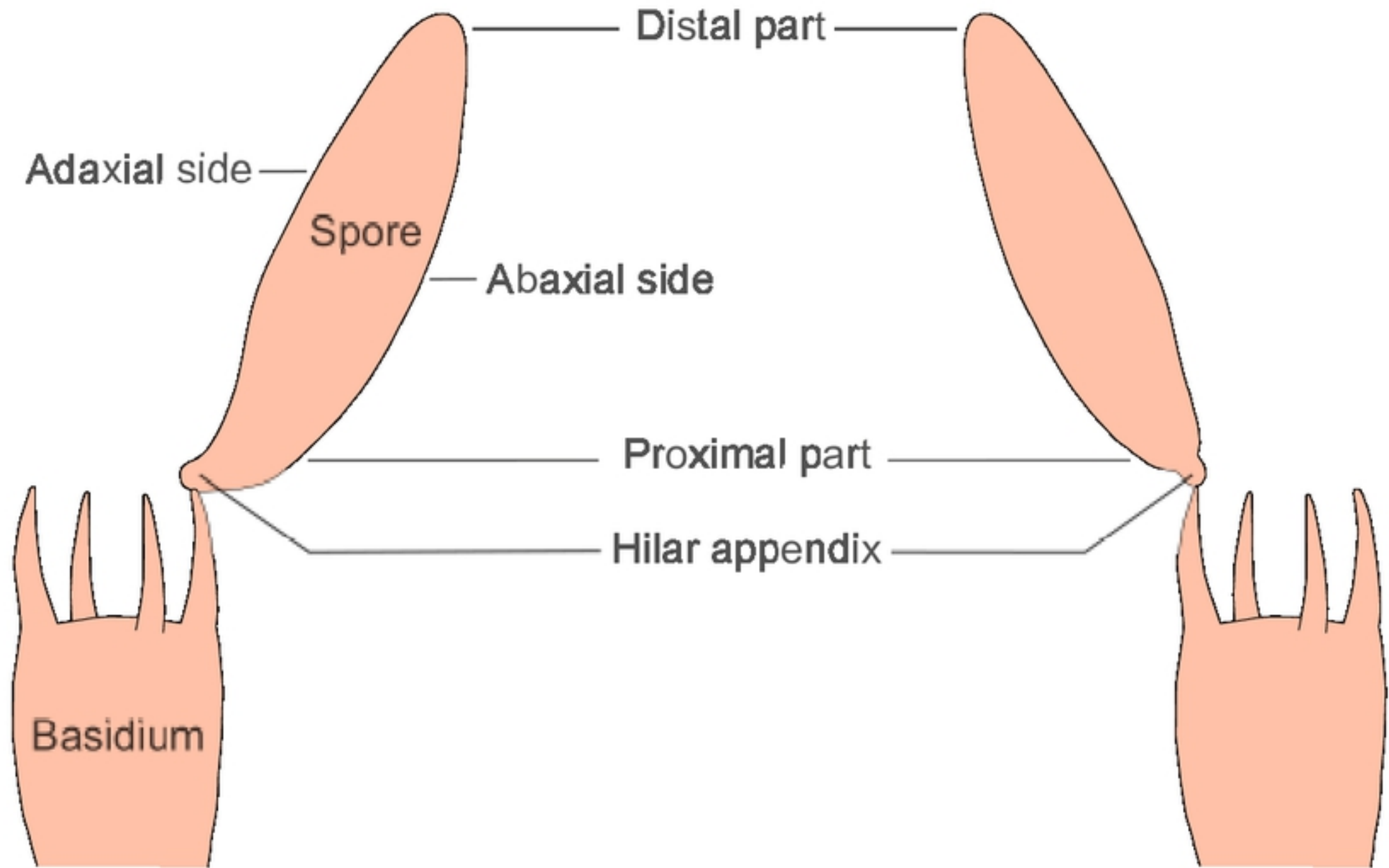


Fig 1



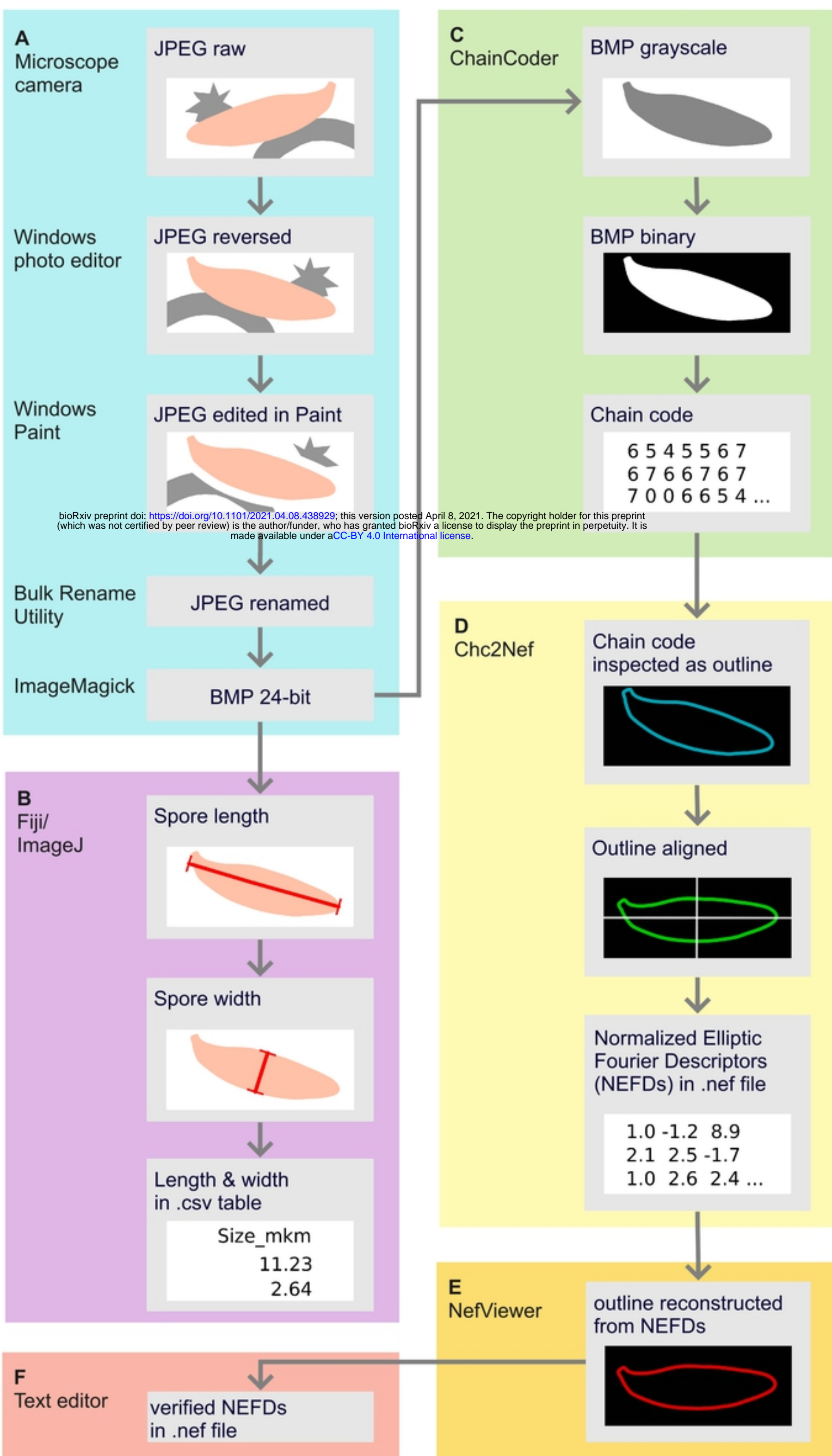


Fig 2

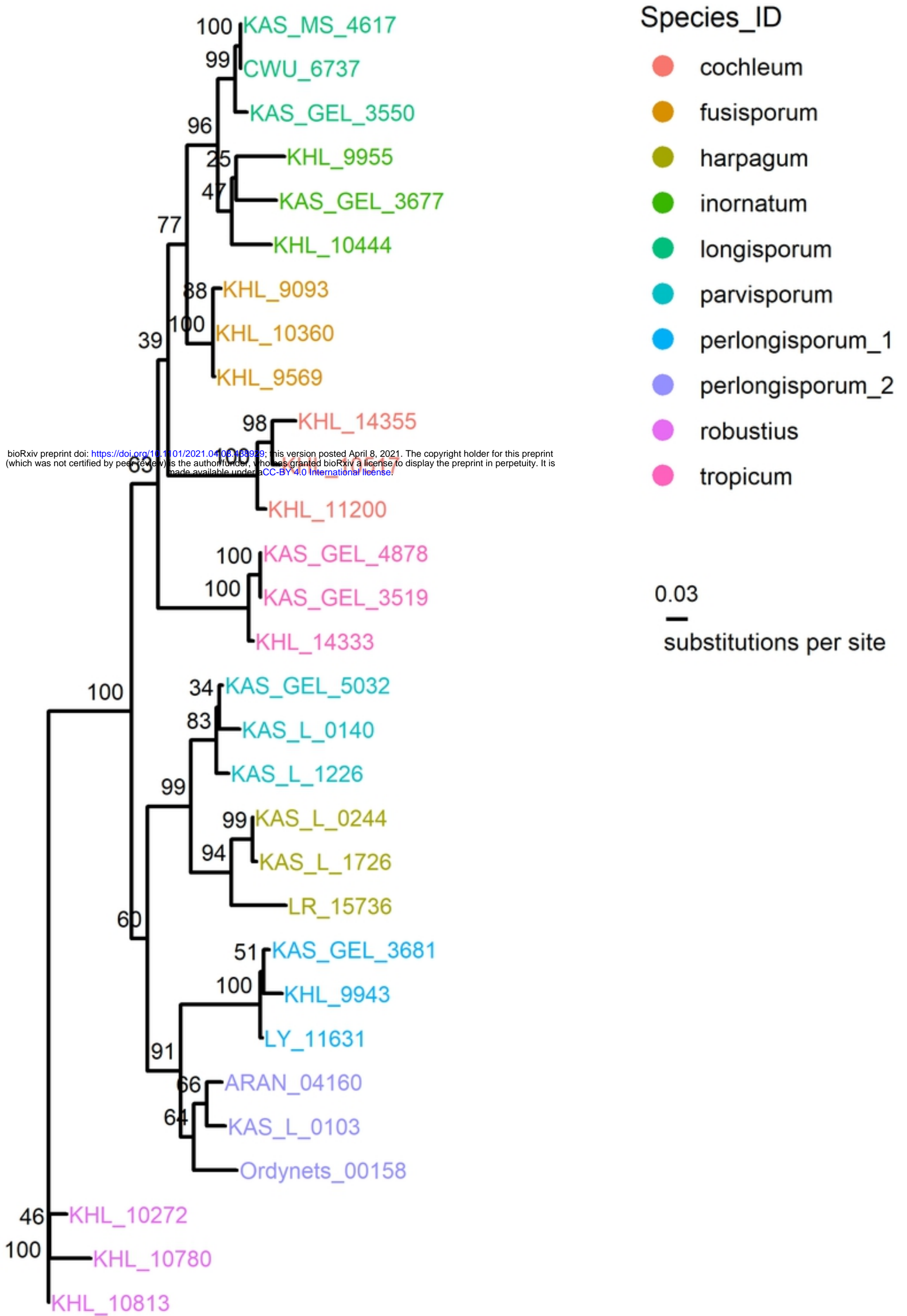


Fig 3

Mean-2SD

Mean

Mean+2SD

Symmetric  
shape  
variation

PC1



bioRxiv preprint doi: <https://doi.org/10.1101/2021.04.08.438929>; this version posted April 8, 2021. The copyright holder for this preprint (which was not certified by peer review) is the author/funder, who has granted bioRxiv a license to display the preprint in perpetuity. It is made available under aCC-BY 4.0 International license.

Asymmetric  
shape  
variation

PC1



PC2

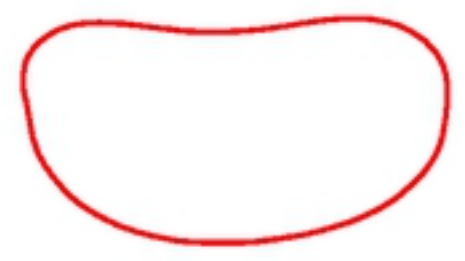


PC3



Global  
shape  
variation

PC1



PC2



Fig 4

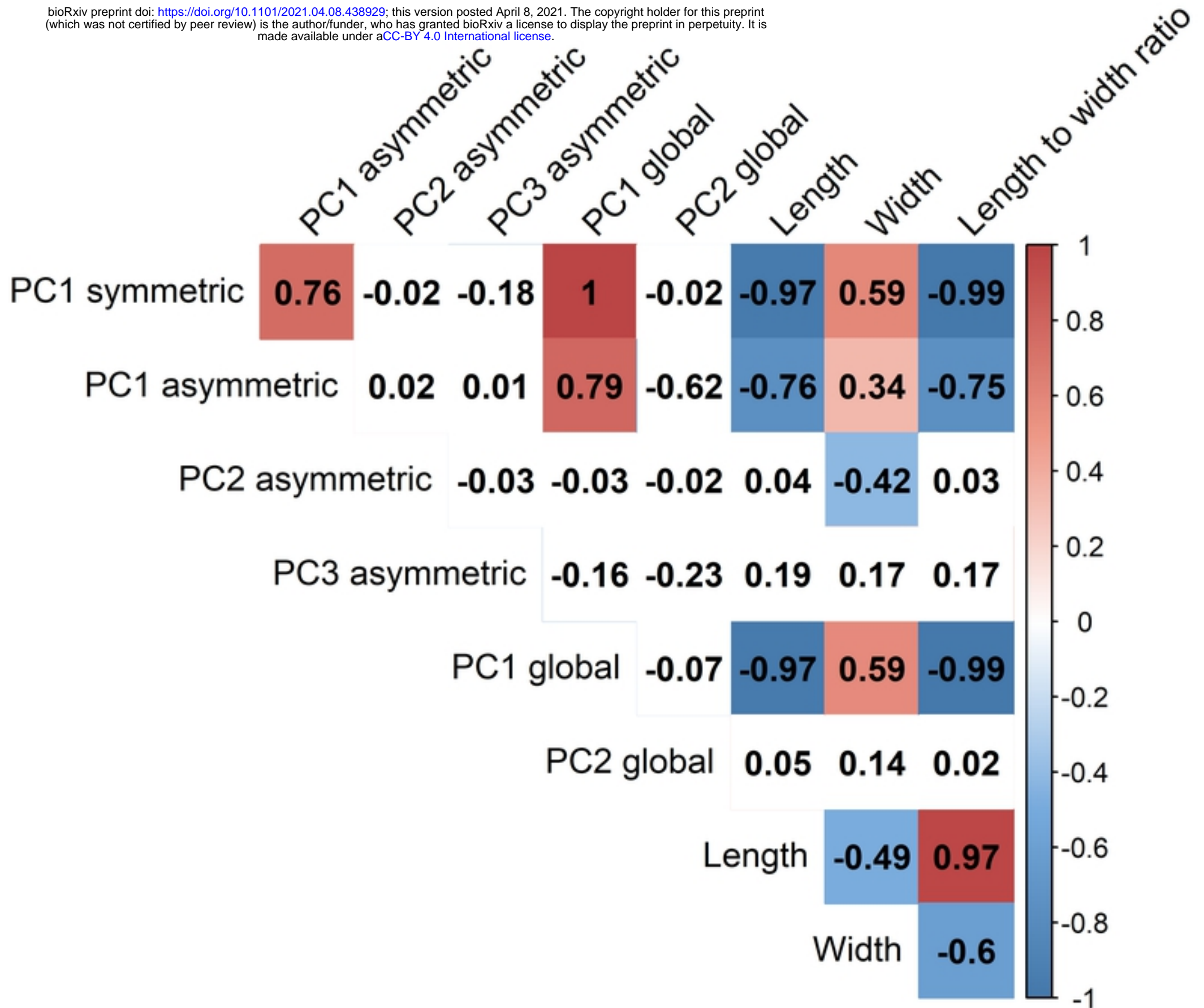


Fig 5